Current Biology, Vol. 14, 145–149, January 20, 2004, ©2004 Elsevier Science Ltd. All rights reserved. DOI 10.1016/j.cub.2004.01.004

The Actin-Interacting Protein AIP1 Is Essential for Actin Organization and Plant Development

Tijs Ketelaar,[1,4] Ellen G. Allwood,[1,4] Richard Anthony,[2] Boris Voigt,[3] Diedrik Menzel,[3] and Patrick J. Hussey[1,*]
[1]The Integrative Cell Biology Laboratory
School of Biological and Biomedical Sciences
University of Durham
South Road
Durham, DH1 3LE
UK
[2]School of Biological Sciences
Royal Holloway University of London
Egham, Surrey, TW20 0EX
UK
[3]University of Bonn
Institute of Botany
Kirschallee 1
D-53115 Bonn
Germany

Summary

Cell division, growth, and cytoplasmic organization require a dynamic actin cytoskeleton. The filamentous actin (F-actin) network is regulated by actin binding proteins that modulate actin dynamics. These actin binding proteins often have cooperative interactions [1, 2]. In particular, actin interacting protein 1 (AIP1) is capable of capping F-actin and enhancing the activity of the small actin modulating protein, actin depolymerising factor (ADF) in vitro [1, 3]. Here, we analyze the effect of the inducible expression of AIP1 RNAi in *Arabidopsis* plants to assess AIP1s role in vivo. In intercalary growing cells, the normal actin organization is disrupted, and thick bundles of actin appear in the cytoplasm. Moreover, in root hairs, there is the unusual appearance of actin cables ramifying the root hair tip. We suggest that the reduction in AIP1 results in a decrease in F-actin turnover and the promotion of actin bundling. This distortion of the actin cytoskeleton causes severe plant developmental abnormalities. After induction of the *Arabidopis* RNAi lines, the cells in the leaves, roots, and shoots fail to expand normally, and in the severest phenotypes, the plants die. Our data suggest that AIP1 is essential for the normal functioning of the actin cytoskeleton in plant development.

Results and Discussion

There are two *AIP1* genes in *Arabidopsis* [3], and a conserved DNA fragment (74%) was used to generate an RNA interference (RNAi) construct controlled by an alcohol inducible promoter [4]. The construct was stably introduced into *Arabidopsis* plants by Agrobacterium-mediated transformation. Selection was on kanamycin, and all positive lines were screened for their response to watering with 0.5% ethanol in soil and reduction in expression of AIP1 by immunoblotting. Selected lines were selfed and the T2 seed used in the experiments.

Four lines that are representative of the range of phenotypes of the soil grown plants were analyzed, AIP1 RNAi lines 1–4 (Figure 1), with the number of each line reflecting the severity of the phenotype with $1 > 2 > 3 > 4$. The effects on aerial organ development were analyzed by watering 3-week-old AIP1 RNAi plants in soil with 25 ml of 0.5% ethanol or water for the controls. 10 days after the start of ethanol induction, growth of leaves, shoots, and flowers was reduced (Figure 1). In the more severe phenotypes, AIP1 RNAi 3 and 4, the plants failed to shoot and flower, the leaves turned brown (indicative of a severe stress response), and continued exposure to ethanol induction resulted in plant lethality (see also Supplemental Data). We tested for the inhibition of AIP1 expression by analyzing total protein extracts by immunoblotting using anti-AIP1. The data showed that the phenotypes shown in Figure 1 correlated with the levels of AIP1 expression, with the lowest levels being in the more severe phenotypes, AIP1 RNAi 3 and 4 (Figure 2).

Germinating the seeds on M and S modified 1B agar plates containing 0.25% ethanol revealed that roots were also affected: root growth was impaired, root hair expansion was decreased, and the density of root hairs was reduced. The phenotypes of the roots across the four RNAi lines were more variable (Figure 3) than the aerial tissues (Figure 1), but the general pattern was the same, i.e., the most severe phenotypes in the two lines (RNAi lines 3 and 4) that express the lowest levels of AIP1.

To ascertain whether the decreased growth was due to a reduction in cell division or cell expansion, we measured the surface area of leaf epidermal cells in RNAi lines as a percentage of similar wild-type cells and the surface area of whole leaves in RNAi plants as a percentage of that of wild-type leaves. If the ratio of the percentages of leaf area to epidermal cell area is one, as will be the case in the wild-type since this is the base parameter, there is no net increase in cell number or cell size. If less than one, this fraction will represent the proportion of the difference in leaf surface area of RNAi lines when compared to wild-type plants caused by smaller cell sizes, e.g., 0.81 or 81% of the leaf in RNAi 4 plants (Table 1). This would suggest that 0.19 or 19% of the decreased growth in RNAi 4 is due to lack of new cell divisions. To further support these data, we measured the growth rate of cells that are typically used as a model for cell expansion studies, the tip-growing root hair cells. Root hair growth rates were up to 5-fold reduced in the RNAi lines, from $1.47 \pm 0.20\ \mu m/min^{-1}$ in the control root hairs to $0.38 \pm 0.19 \mu m/min^{-1}$ in the RNAi 3 line, which shows the most severe root hair phenotype (Figure 3). These data demonstrate that the decreased growth is caused principally by an overall reduction in cell expansion. Some cell types, e.g., trichomes and stomata (compare Figure 4A with 4C) are not affected after induction by

*Correspondence: p.j.hussey@durham.ac.uk
[4]These authors contributed equally to this work.

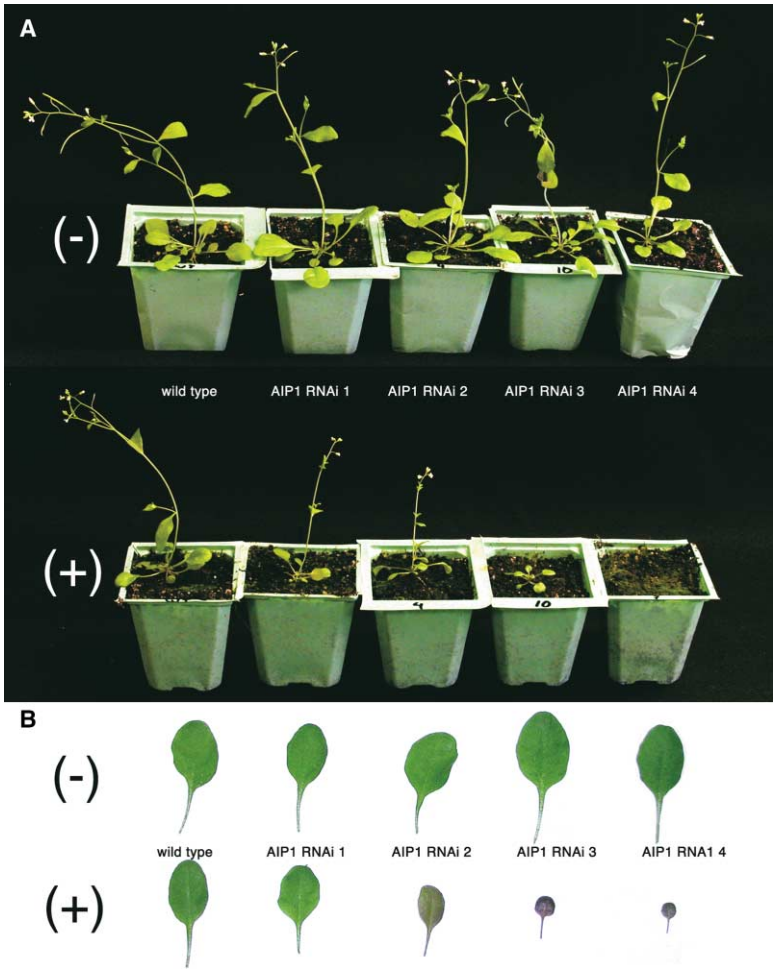

Figure 1. Aerial Organs of AIP1 RNAi Lines 1–4

(A) Plants grown in soil without (−) or with (+) induction by watering with 0.5% ethanol. (B) A comparison of the sixth leaf of each line without (−) or with (+) induction.

ethanol; however, we could not determine whether the RNAi was active in these cell types.

AIP1 was first identified in yeast in a two-hybrid screen using actin as the bait [5]. Mutations in *AIP1* cause defects in actin organization in *Caenorhabditis elegans*, but these mutations are not lethal [6]. We examined the effects on actin filament organization in the AIP1 RNAi lines during ethanol induction. We generated *Arabidopsis* plants expressing a chimeric gene fusion of green fluorescent protein and the second actin binding domain of *Arabidopsis* fimbrin 1 (GFP:FABD) for marking the actin network. Expressing this construct in *Arabidopsis* had no observable effect on actin organization or plant growth and development. The GFP:FABD was crossed into the AIP1 RNAi lines, which allowed the visualization of the actin cytoskeleton during alcohol induced inhibition of AIP1 expression.

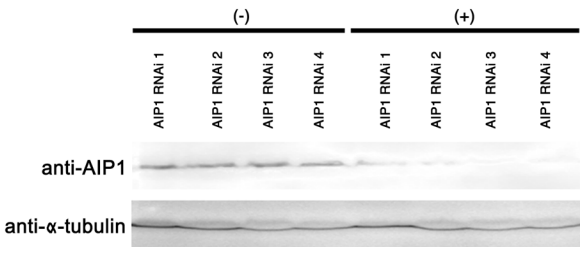

Figure 2. AIP1 Expression in AIP1 RNAi Lines 1–4

Immunoblot of total protein extracts from AIP1 RNAi plants. The same immunoblot probed with anti-AIP1, followed by anti-α tubulin as control. (−), without induction; (+), with induction.

Dramatic differences in actin configuration between the uninduced and induced AIP1 RNAi /GFP:FABD lines were observed (Figure 4). No effects on the actin organization in plant cells expressing GFP:FABD watered with 0.5% ethanol were observed (Figures 4B and E). The data shown in Figure 4 are for RNAi line 4 representing the severest phenotype in the aerial parts of the plants and RNAi line 3 for the severest root hair phenotypes. The actin cytoskeleton in intercalary expanding cell types of the induced plants was organized into thicker and more compact bundles than in the uninduced plants (compare Figure 4A and 4C). Root hairs are tip-growing cells that are normally very sensitive to changes in the actin cytoskeleton during development [7]. In elongating root hairs, F-actin permeates the cytoplasm with F-actin bundles parallel to the long axis of the hair. F-actin bundles are not observed extending into the apex (Movie 1 and Figure 4D). In contrast in the induced AIP1 RNAi/ GFP:FABD lines, F-actin bundles are present in the short root hairs and these extend into the apex (Movie 2 and

Table 1. Surface Area of AIP RNAi 1–4 Cells and Leaves Given as Percentages of Wild-Type Cell Surface Area and Leaf Surface Area

	Wild-Type	AIP1 RNAi 1	AIP1-RNAi 2	AIP1 RNAi 3	AIP1 RNAi 4
Cell surface area (%)	100 (±9.1)	103 (±8.3)	56 (±8.6)	26 (±3.7)	20 (±4.2)
Leaf surface area (%)	100 (±8.3)	99 (±7.1)	53 (±7.6)	22 (±4.0)	16 (±4.2)
Ratio of leaf/cell	1	0.95	0.95	0.85	0.81

The ratio between leaf surface area and cell surface area represents the fraction of leaf surface area that can be accounted for by the reduction in cell surface area.

Figure 4F). This was observed in every root hair examined.

In this paper, we have shown that the inhibition of AIP1 gene expression causes disruption of normal actin organization and plant development. Thick bundles of actin appear in intercalary expanding cells and in the tip-growing root hairs actin cables protrude into the apices. These defects in actin organization correlate

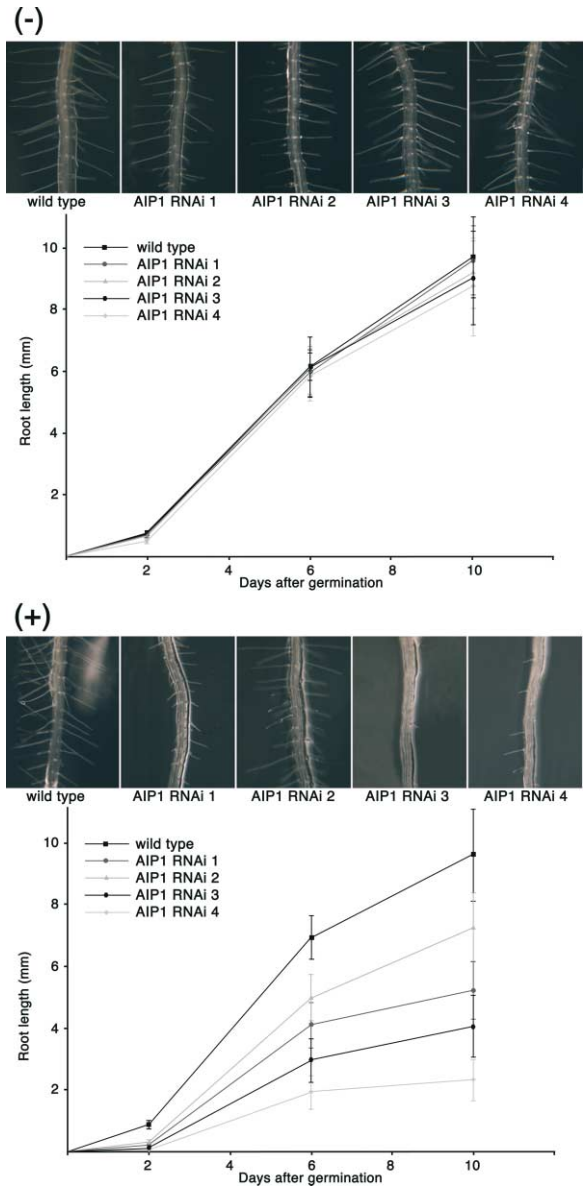

Figure 3. Roots of AIP1 RNAi Lines 1–4

Roots and root hairs, and the length of roots from AIP RNAi lines grown on plates in the absence (−) or presence (+) of 0.25% ethanol.

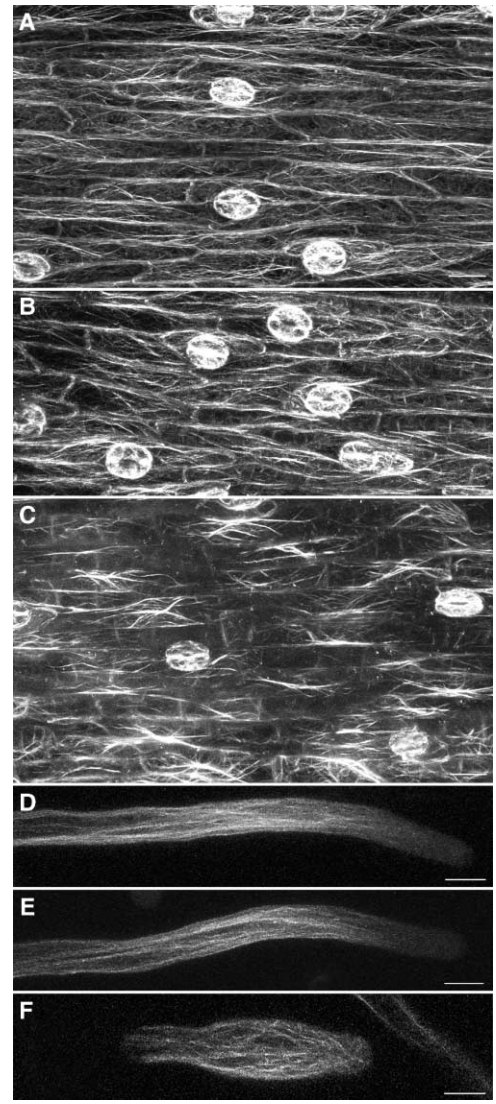

Figure 4. The Actin Cytoskeleton in AIP1 RNAi Lines and GFP:FABD Plants

(A–C) Shoot epidermal cells. (A) AIP1 RNAi line 3 without (−) induction. (B) GFP:FABP watered with 0.5% ethanol (control). (C) AIP1 RNAi line 3 with (+) induction by 0.5% ethanol.

(D–F) Growing root hairs. (D) AIP RNAi line 3 without (−) induction. (E) GFP:FABD watered with 0.5% ethanol. (F) AIP1 RNAi line 3 with (+) induction by 0.5% ethanol.

Scalebars represent 50 μm in (A)–(C) and 10 μm in (D)–(F).

with the breakdown of normal plant development: leaves do not expand, shoots and roots either fail to form or are stunted, root hairs grow only slowly, and as the plants do not bolt, there is no flowering in the severest phenotypes, which die.

The appearance of F-actin bundles would suggest that actin is being stabilized. The fact that the cells do not expand would imply that no extra polymerization is taking place, as actin polymerization is required for cell expansion in plant cells. This is concluded from the fact that cell expansion is inhibited by actin-depolymerizing drugs [8] and also that the cells are small in plants underexpressing profilin [9]. In contrast underexpressing ADF in plants results in increased cell growth [10]. In vitro ADF and profilin can act synergistically to increase F-actin turnover [11], but in terms of plant development their activity is antagonistic [9, 10]. It would seem that this is also the case with AIP1 and ADF: ADF and AIP1 synergistically increase actin dynamics in vitro, but in plant development their activity appears antagonistic. It is likely that a fine balance in their respective activities is necessary.

AIP1 enhances actin depolymerization by ADF in vitro [3, 12, 13, 14]. Moreover, it has been shown that AIP1 caps the plus or barbed end of actin filaments decorated with actin depolymerizing factor [15]. This capping inhibits polymerization at the barbed ends of filaments but does not inhibit the F-actin severing activity or the promotion of minus end depolymerization activity of ADF. Therefore, the enhanced actin depolymerization/severing activity of AIP1 in combination with ADF has been hypothesized to be caused by the inability of AIP1 capped filaments to elongate and to reanneal, leading to increased actin depolymerization at the pointed ends of the fragments [1]. This in vitro activity can be used to explain the appearance of F-actin bundles in the AIP1 RNAi plants. Depletion of AIP1 will result in reduced disassembly of actin filaments and a decrease in the turnover of actin filaments: the filaments are less dynamic. In addition, reducing AIP1 levels could potentially result in increased assembly because the barbed end is now available for polymerization. In the apex of root hairs where actin dynamics are high [7, 16] there are no bundles of actin, but when AIP1 is depleted, bundles of actin protrude into this region. This would suggest that the net affect of AIP1 depletion is a reduction in the turnover of F-actin and that this facilitates actin bundling by as yet unknown actin bundling proteins.

The phenotype of the AIP1 depleted plants is more severe than the null mutants *unc-78* in *C. elegans* [6], DAip1 in *Dictyostelium discoideum* [17], and *aip1* in *Saccharomyces cerevisiae* [13]. The *unc-78* null mutation causes appearance of actin aggregates in muscle and is defective in muscle contractile activity. The DAip1 null cells are impaired in growth, cytokinesis, fluid phase uptake, phagocytosis, and cell movement. Deletion of Aip1p in yeast does not affect growth, and there are no discernable morphological defects. It is unclear why depletion of AIP1 has such a severe affect on overall plant development. However, it could reflect the differences in the mechanisms of development between plants and these other organisms. For example, the major difference between plant and animal development is that plant cells cannot move so organ development is dependent on the balance of cell expansion and cell division. If this balance is disrupted, then plant development will either be impaired or not take place at all. The data in this paper have shown that AIP1 is essential for plant cell expansion and subsequent plant growth and development.

Experimental Procedures

Constructs and Plant Transformation

AIP1 RNAI Vector

The AIP RNAi vector was constructed using the invert hairpin loop method [18]. The most conserved region (74%) of the two plant AIP1 genes that does not include the WD repeats is in the 5′ region of the sequence. The sense fragment covering the first 836 bp was generated by PCR from AtAIP1-1 [3] incorporating BamHI-SalI/SacI ends. The antisense fragment was generated, also by PCR, from the 553 bp region proximal to the 3′ region of the sense fragment with BamH1/Sal1 ends. The sense and antisense fragments were joined in pGEMT (Promega). The resulting cassettes were excised using Sal I and subcloned into the SalI site of palcA:CAT [4]. This results in a replacement of the CAT cassette. The alcA:AIPRNAi:nos cassette was finally subcloned into the p35S:alcR vector [4].

GFP:FABD vector

The carboxy terminal region, 325–687 bp, harboring the actin binding domain of AtFIM1 [19] was cloned in frame into pCATgfp [20], which was modified to abolish the GFP termination codon. The expression cassette with the fused GFP:Fimbrin1 Actin Binding Domain 2 sequence together with the 35S promoter was excised by Sse8387I and inserted into the Pst1 site of the binary vector pCB302 [21].

Transformation

The alcohol inducible AIP1 RNAi vector or the GFP:FABD vector was transferred to *Agrobacterium tumefaciens* strain GV3101 (pMP90) and used to transform *Arabidopsis* ecotype Col-0 by floral dipping [22]. Positive lines were either selected on 50 mg/L kanamycin plates (AIP1 RNAi vector) or by screening for green fluorescent seedlings (GFP:FABD vector).

Protein Extraction, Electrophoresis, and Immunoblotting

Protein extraction, electrophoresis, and protein gel blot analysis were carried out as described previously [3].

Plant Material

Wild-type *Arabidopsis* Col-0 was used in the controls. AtAIP1 RNAi 1, 2, 3, and 4 plants were selected as representatives of the kanamycin positive seed based on their phenotype after ethanol induction, and T2 seed was used throughout. *Arabidopsis* T3 seeds harboring GFP:FABD were used for crossing to AtAIP1 RNAi lines. Seeds were potted in general purpose compost and sand (4:1) and grown in a glass house. After 3 weeks, the AIP1 RNAi plants were fed with 25 ml of 0.5% ethanol every 3 days, and the phenotypes were recorded. To observe the effects on root development, seeds were surface sterilized by soaking in 10% bleach plus 0.05% Triton X-100 for 15 min, followed by three washes in sterile distilled water. Subsequently, the seeds were germinated on top of coverslips with a thin layer of solid medium [23] covered with biofilm (Vivascience via Merck, Poole, UK). 0.7% Plant agar (Duchefa, Haarlem, The Netherlands) was used to solidify the medium. The slides with seedlings were contained in 70 mm petridishes wrapped with parafilm. Plants were cultured at 22°C in a long daylight regime (16 hr light, 8 hr dark) for 5 days. The AIP1 RNAi was induced by addition of 0.25% ethanol to the medium.

Calculations

For all measurements in Table 1, the sixth leaf from the rosette was taken after 10 days induction with ethanol (see above). At least 60 epidermal cell surface measurements equally divided over six different leaves from the same line were taken and these from two random areas of each leaf. Leaf surface area was determined using at least 12 sixth leaf leaves for each line.

Microscopy

Confocal imaging was performed on a Zeiss LSM510 META system. The Argon-ion laser was used at 4% of the maximum power for imaging, combined with main dichroic beamsplitter HFT 488 nm and a BP 505–530 nm emission filter.

Supplemental Data

Supplemental data including two movies and experimental procedures are available at htttp://www.current-biology.com/cgi/content/full/14/2/145/DC1/.

Acknowledgments

This work was funded by the Biotechnology and Biological Sciences Research Council, UK. (TK, EGA and PJH).

Received: November 19, 2003
Revised: December 8, 2003
Accepted: December 9, 2003
Published: January 20, 2004

References

1. Ono, S. (2003). Regulation of actin filament dynamics by actin depolymerizing factor/cofilin and the actin-interacting protein 1: new blades for twisted filaments. Biochemistry *42*, 13363–13370.
2. Ayscough, K.R. (1998). *In vivo* functions of actin-binding proteins. Curr. Opin. Cell Biol. *10*, 102–111.
3. Allwood, E.G., Anthony, R.G., Smertenko, A.P., Reichelt, S., Drobak, B.K., Doonan, J.H., Weeds, A.G., and Hussey, P.J. (2002). Regulation of the pollen-specific actin-depolymerizing factor LIADF1. Plant Cell *14*, 2915–2927.
4. Caddick, M.X., Greenland, A.J., Jepson, I., Krause, K.P., Qu, N., Riddell, K.V., Salter, M.G., Schuch, W., Sonnewald, U., and Tomsett, A.B. (1998). An ethanol inducible gene switch for plants used to manipulate carbon metabolism. Nat. Biotechnol. *16*, 177–180.
5. Amberg, D.C., Basart, E., and Botstein, D. (1995). Defining protein interactions with yeast actin in-vivo. Nat. Struct. Biol. *2*, 28–35.
6. Ono, S. (2001). The *Caenorhabditis elegans* unc-78 gene encodes a homologue of actin-interacting protein 1 required for organized assembly of muscle actin filaments. J. Cell Biol. *152*, 1313–1319.
7. Ketelaar, T., De Ruijter, N.C.A., and Emons, A.M.C. (2003). Unstable F-actin specifies area and microtubules direction of cell expansion in Arabidopsis root hairs. Plant Cell *15*, 285–292.
8. Baluska, F., Jasik, J., Edelmann, H.F., Salajov á, T., and Volkmann, D. (2001). Latrunculin B-induced plant dwarfism: plant cell elongation is F-actin-dependent. Dev. Biol. *231*, 113–124.
9. Ramachandran, S., Christensen, H.E.M., Ishimaru, Y., Dong, C.-H., Chao-Ming, W., Cleary, A.L., and Chua, N.-H. (2000). Profilin plays a role in cell elongation, cell shape maintenance, and flowering in Arabidopsis. Plant Physiol. *124*, 1637–1647.
10. Dong, C.H., Xia, G.X., Hong, Y., Ramachandran, S., Kost, B., and Chua, N.H. (2001). ADF proteins are involved in the control of flowering and regulate F-actin organization, cell expansion, and organ growth in Arabidopsis. Plant Cell *13*, 1333–1346.
11. Didry, D., Carlier, M.F., and Pantaloni, D. (1998). Synergy between actin depolymerizing factor/cofilin and profilin in increasing actin filament turnover. J. Biol. Chem. *273*, 25602–25611.
12. Okada, K., Obinata, T., and Abe, H. (1999). XAIP1: a Xenopus homologue of yeast actin interacting protein (AIP1), which induces disassembly of actin filaments cooperatively with ADF cofilin family proteins. J. Cell Sci. *112*, 1553–1565.
13. Rodal, A.A., Tetreault, J.W., Lappalainen, P., Drubin, D.G., and Amberg, D.C. (1999). Aip1p interacts with cofilin to disassemble actin filaments. J. Cell Biol. *145*, 1251–1264.
14. Aizawa, H., Katadae, M., Maruya, M., Sameshima, M., Murakami-Murofushi, K., and Yahara, I. (1999). Hyperosmotic stress-induced reorganization of actin bundles in Dictyostelium cells over-expressing cofilin. Genes Cells *4*, 311–324.
15. Okada, K., Blanchoin, L., Abe, H., Chen, H., Pollard, T.D., and Bamburg, J.R. (2002). Xenopus actin-interacting protein 1 (XAip1) enhances cofilin fragmentation of filaments by capping filament ends. J. Biol. Chem. *277*, 43011–43016.
16. Miller, D.D., De Ruijter, N.C.A., Bisseling, T., and Emons, A.M.C. (1999). The role of actin in root hair morphogenesis: studies with lipochito-oligosaccharide as a growth stimulator and cytochalasin as an actin perturbing drug. Plant J. *17*, 141–154.
17. Konzok, A., Weber, I., Simmeth, E., Hacker, U., Maniak, M., and Muller-Taubenberger, A. (1999). DAip1, a Dictyostelium homologue of the yeast actin-interacting protein *1*, is involved in endocytosis, cytokinesis, and motility. J. Cell Biol. *146*, 453–464.
18. Vance, V., and Vaucheret, H. (2001). RNA silencing in plants: defense and counterdefense. Science *292*, 2277–2280.
19. McCurdy, D.W., and Kim, M. (1998). Molecular cloning of a novel fimbrin-like cDNA from *Arabidopsis thaliana*. Plant Mol. Biol. *36*, 23–31.
20. Reichel, C., Mathur, J., Eckes, P., Langenkemper, K., Koncz, C., Schell, J., Reiss, B., and Maas, C. (1996). Enhanced green fluorescence by the expression of an *Aequorea victoria* green fluorescent protein mutant in mono- and dicotyledonous plant cells. Proc. Natl. Acad. Sci. USA *93*, 5888–5893.
21. Xiang, C., Han, P., Lutziger, I., Wang, K., and Oliver, D.J. (1999). A mini binary vector series for plant transformation. Plant Mol. Biol. *40*, 711–717.
22. Clough, S.J., and Bent, A.F. (1998). Floral dip: a simplified method for Agrobacterium-mediated transformation of *Arabidopsis thaliana*. Plant J. *16*, 735–743.
23. Wymer, C.L., Bibikova, T.N., and Gilroy, S. (1997). Cytoplasmic free calcium distributions during the development of root hairs of *Arabidopsis thaliana*. Plant J. *12*, 427–439.